Study of a Fatty Acid Binding Site of Interphotoreceptor Retinoid-Binding Protein Using Fluorescent Fatty Acids

Tatiana Putilina,* David Sittenfeld, Gerald J. Chader, and Barbara Wiggert

Laboratory of Retinal Cell and Molecular Biology, National Eye Institute, National Institutes of Health, Bethesda, Maryland 20892

Received August 31, 1992; Revised Manuscript Received January 28, 1993

ABSTRACT: Interphotoreceptor retinoid-binding protein (IRBP) is a 140-kDa glycolipoprotein which constitutes about 70% of the soluble protein of the retinal interphotoreceptor matrix. Much is known concerning its role in the transport of retinoids between photoreceptor cells and pigment epithelium but little is known about its interactions with lipids. Here we have examined the physicochemical characteristics of a fatty acid binding site of IRBP using a set of fluorescent fatty acid analogs with an anthracene moiety attached at different positions along the hydrocarbon chain. The results show that fatty acids are bound in a hydrophobic environment as indicated by a blue shift in fluorescence maxima and by a increase in quantum yield of the bound ligand. There is a single specific fatty acid binding site for each molecule of IRBP with an apparent $K_d = 3.6 \times 10^{-7}$ M. There is a nonradiative energy transfer from tryptophan residues to bound ligand. The interactions of IRBP and bound fatty acid are sensitive to denaturation by increasing concentrations of urea as judged by changes in nonradiative energy transfer efficiency and the quantum yield of bound probe. Quantum yields of bound fatty acid analogs varied with position of the fluorophore along the hydrocarbon chain and had the lowest values for the fluorophore located at the midpoint. Probing of the microenvironment of bound fluorophore with a quencher indicated a highly structured binding site.

The interphotoreceptor matrix (IPM)[1] is a layer of extracellular, protein-rich, and highly-organized material between the retinal photoreceptor neurons and the pigment epithelial cell layer. In the visual cycle, retinoids travel across this matrix in response to cycles of light and dark (Dowling, 1960). Interphotoreceptor retinoid-binding protein (IRBP) is an extracellular, retinoid-binding protein that mediates transport of retinoids in the IPM (Okajima et al., 1989, 1990; Carlson & Bok, 1992) as well as protecting the retinoids from isomerization and oxidative damage (Crouch et al., 1992).

In addition to facilitation of retinoid transit, IRBP has been shown to bind up to 90% of the fatty acids in monkey IPM (Bazan et al., 1985). The endogenous fatty acid composition of purified IRBP is very high (6.5 mol/mol of IRBP) and is different from that of intracellular proteins involved in lipid transport or metabolism (Bazan et al., 1985). It is not clear whether IRBP simply aids solubilization of hydrophobic ligands or plays a regulatory role in intercellular metabolism. It is conceivable that fatty acids may have a modulatory effect on what is considered to be a major function of IRBP, i.e., retinoid binding and transport. It is not unique for a protein to be able to bind more than one hydrophobic ligand noncovalently (Glatz et al., 1990). Interference with the binding of another ligand by fatty acids has been reported for cellular retinoic acid-binding protein (CRABP) (Sani et al., 1987), sex steroid binding protein (SBP) (Martin et al., 1985), and rat liver glucocorticoid receptors (Vallette et al., 1991). On the other hand, IRBP's large size and its elongated shape (axial ratio of 8:1; Adler et al., 1985) may allow for the existence of independent fatty acid binding sites, providing it with an additional physiological role as an intercellular fatty acid carrier. Little information is available, however, regarding the physical and chemical characteristics of fatty acid binding sites of IRBP or their possible interactions with a retinol binding sites. Binding sites of fatty acid binding proteins (FABPs) have been studied for some time using fluorescent fatty acid analogs (Storch et al., 1989; Storch, 1990; Wootan et al., 1990). In this report, fluorescent anthroyloxy analogs (AOffa) of stearic and palmitic acids were used to probe the fatty acid binding site of IRBP. These fatty acid analogs have the fluorescent moiety attached at different positions along the carbon chain; however, their intrinsic properties remain the same (Thulborn et al., 1987), allowing us not only to examine the general characteristics of fatty acid binding to IRBP but also to probe the microenvironment in different parts of the protein.

EXPERIMENTAL PROCEDURES

Materials. IRBP was purified from light-adapted bovine eyes using procedures described elsewhere (Pepperberg et al., 1991). It is essentially retinoid-free under these conditions. The fluorescent probes of the C-16 (palmitate) and C-18 (stearate) fatty acids as 2- and 16-(9-anthroyloxy)palmitic acid (2-AP and 16-AP) and 2-, 3-, 6-, 7-, 9-, 10-, and 12-(9-anthroyloxy)stearic acid (2-AS, 3-AS, etc.) were obtained from Molecular Probes Inc. (Eugene, OR).

Binding of AOffa to IRBP. Experiments were performed in 1- × 1-cm quartz cuvettes in phosphate-buffered saline (PBS), pH 7.2, at room temperature unless otherwise specified. IRBP solution (2.5 mL, approximately 0.6 μM) was titrated with small increments (5–10 μL) of the ligand in ethanol. The amount of ligand was chosen to cover the range of ligand: protein ratio up to about 3:1. Following each addition of ligand, the solution was mixed and allowed to equilibrate for 5 min. Free AOffa can form a micellar structure (Cogan et al., 1976) which appears as a slow rise in background fluorescence. This effect is more pronounced at higher AOffa

[1] Abbreviations: IRBP, interphotoreceptor retinoid-binding protein; IPM, interphotoreceptor matrix; FABP, fatty acid-binding protein; AOffa, anthroyloxy free fatty acid; ffa, free fatty acid; PBS, phosphate-buffered saline; AS (anthroyloxy)stearic acid; AP, (anthroyloxy)palmitic acid; PE, pigment epithelium.

This article not subject to U.S. Copyright. Published 1993 by the American Chemical Society

concentrations; therefore, it is important to keep the time of equilibration constant. At the end of each titration experiment, the ethanol concentration did not exceed 3%. Fluorescence intensities were measured using a SLM Aminco SPF-500C spectrofluorometer (SLM Instruments, Inc., Urbana, IL). The SPF-500C spectrofluorometer operates in a ratio mode, using a xenon light source which is filtered through excitation and emission monochromators. Wavelengths of excitation and emission were 360 and 454 nm. Fluorescence intensities were corrected for the fluorescence contribution of free ligand and the number of binding sites and their affinities were calculated according to the method of Cogan et al. (1976). Using this method, the concentration of free ligand is not measured directly. Instead, the fraction of free binding sites (α) is calculated for every desired point according to the relationship $\alpha = (F_{max}-F)/(F_{max}-F_0)$, where F is the fluorescence intensity at a certain retinol concentration, F_{max} is the fluorescence intensity upon saturation of a protein (P_0) with a ligand (R_0), and F_0 is the initial fluorescence intensity. Concentration of a free ligand, R, was estimated using the relationship $R = R_0 - nP_0(1 - \alpha)$, where n was assumed to equal 1. The corresponding fluorescence of a free ligand was subtracted from a recorded fluorescence intensity and the resulting curve was used to calculate new α values. By plotting $P_0\alpha$ vs $R_0\alpha/(1-\alpha)$, the apparent dissociation constant (K_d) and the number of binding sites (n) are derived from the intercept of K_d/n and the slope of $1/n$.

Steady-State Fluorescence Measurements. Fluorescence emission spectra were corrected for a blank containing all components except AOffa. Excitation and emission slits of 4 nm were used unless otherwise stated. Excitation wavelengths were 360 nm for AOffa, 295 nm for tryptophan, and 352 nm for quinine sulfate. Quantum yields (Q) of bound AOffa were determined relative to quinine sulfate in 0.1 N sulfuric acid (Scott et al., 1970).

The effect of increasing concentrations of urea on the AOffa–IRBP complex was followed by changes in fluorescence emission at 454 nm with excitation at 360 nm. Each sample contained 100 nmol of IRBP and 200 nmol of 16-AP in PBS buffer and increasing concentrations of urea, which was added from an 8 M stock solution in PBS. Fluorescence intensities were corrected for emission due to urea and free fluorophore.

Nonradiative energy transfer from tryptophan residues to a bound AOffa was followed by the decrease in quantum yield of a donor (tryptophan) upon addition of acceptor (AOffa). Wavelengths of excitation and emission were 295 and 335 nm. The efficiency of energy transfer (E) was calculated from its relation to the intensity of donor fluorescence in the absence (F_{od}) and presence (F_d) of the acceptor: $E = 1 - (F_d/F_{od})$.

Fluorescence Quenching by Acrylamide. Quenching experiments were conducted by the addition of small aliquots (10–30 μL) of stock acrylamide solution (5 M in PBS) to 2.5 mL of protein solution. After thorough mixing and equilibration for about 2 min, changes in emission fluorescence were recorded. Wavelengths of excitation and emission were 360 and 454 nm. No corrections for an acrylamide inner effect were necessary at these wavelengths. After corrections for dilutions and for the blank, results were plotted according to the Stern–Volmer equation (Lakowicz, 1983):

$$I_o/I = 1 + K_{SV}[Q]$$

where I_o and I are the fluorescence intensities in the absence and presence of quencher, [Q] is the concentration of a quencher in molar, and K_{SV} is the Stern–Volmer quenching constant.

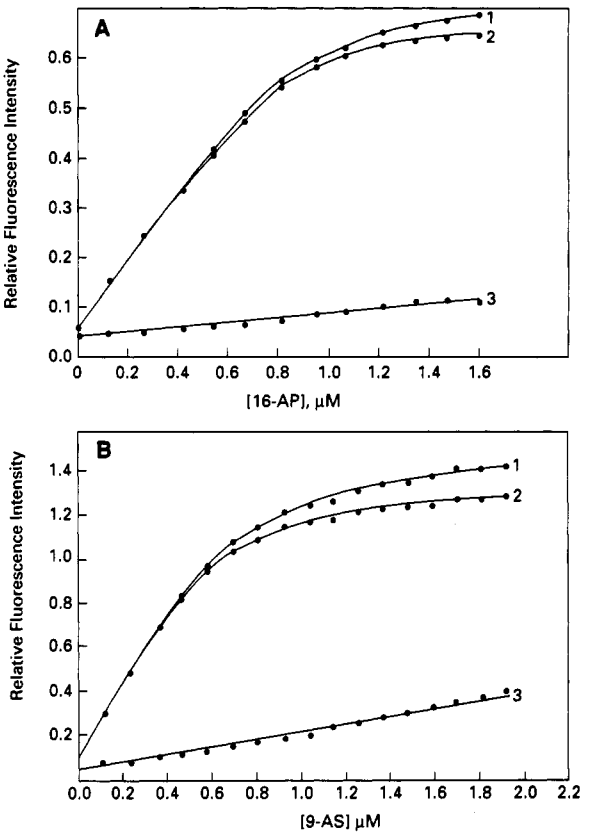

FIGURE 1: Titration of bovine IRBP with 16-(9-anthroyloxy)palmitic acid (A) or 9-(9-anthroyloxy)stearic acid (B) as followed by the increase in fluorescence intensity. Excitation and emission wavelengths were 360 and 454 nm. Curve 1, observed fluorescence intensity; curve 2, fluorescence intensity corrected for unbound AOffa; curve 3, fluorescence intensity of free OAffa in solution.

RESULTS

Binding of AOffa to IRBP. Fluorescence titration curves of IRBP with 16-AP and 9-AS are shown in Figure 1. The titration patterns are very similar for the two ligands, with the half-saturation point at about a 1:1 ratio of protein to AOffa. Apparent saturation of binding occurs above a 2:1 molar ratio. From the intercept and the slope of the straight lines (Figure 2), the apparent dissociation constants of the AOffa/AOffa–protein complexes and the number of binding sites were calculated (Table I). The results indicate similar binding affinities of IRBP for 16-AP and 9-AS with an average value of 3.6×10^{-7} M and a single binding site. As can be seen from Figure 3, at much higher ligand concentrations the fluorescence titration curve appears to reach another plateau at a different ligand to protein ratio. Attempts to calculate the number of binding sites using the Cogan plot suggested a multiple ligand assembly around the IRBP molecule. It is probable that, at such high concentrations of free ligand, a micellar structure is formed in solution (Cogan et al., 1978) or around the protein molecule, making accurate calculations impossible due to deviations from the linear function of the Cogan plot. However, the overall quantum yield increase of the ligand suggests that IRBP facilitates the solubilization of hydrophobic ligands at more than one binding site at a high ligand to protein ratio.

Binding of fluorescent fatty acids can be affected by the presence of docosahexanoic acid (22:6 fatty acid), which is a nonfluorescent fatty acid occurring naturally in the retina

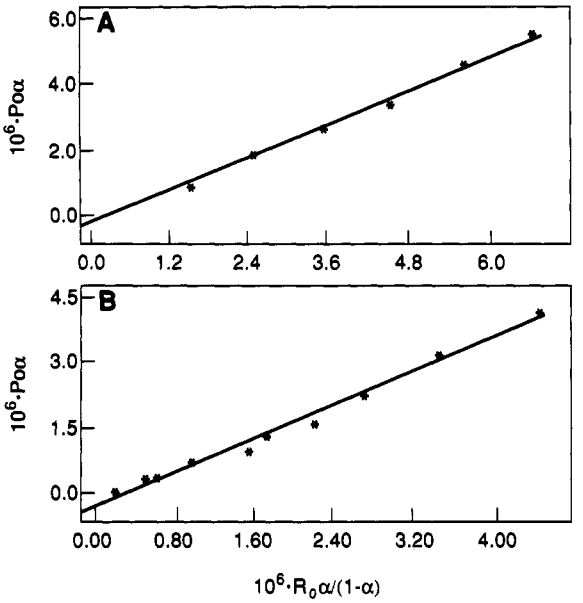

FIGURE 2: Cogan linear least-squares plots for the titration of IRBP with 16-(9-anthroyloxy)palmitic acid (A) or 9-(9-anthroyloxy)stearic acid (B).

Table I: Apparent Dissociation Constants and Apparent Molar Ratios of AOffa/IRBP at Saturation

AOffa	K_d ($\times 10^7$)	n
16-AP	3.55	0.80
9-AS	3.56	0.98

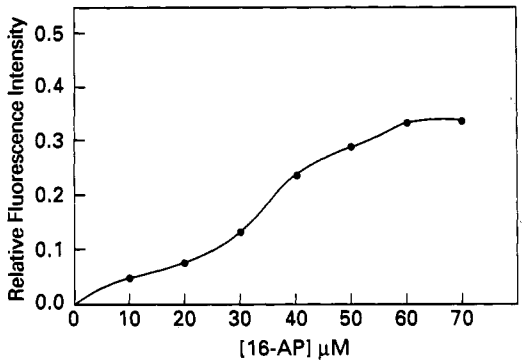

FIGURE 3: Titration of bovine IRBP (10 nM) with 16-AP as followed by the increase in fluorescence intensity. The curve demonstrates nonspecific binding at higher concentrations of ligand. Excitation and emission wavelengths were 360 and 454 nm. Fluorescence intensities were corrected for emission due to a fluorescence of a free ligand in solution.

(Figure 4). As can be seen from the emission spectra, the fluorescence intensity of bound 16-AP decreases approximately 30% after addition of an equimolar amount of 22:6 fatty acid. In a parallel experiment, IRBP was incubated with 22:6 fatty acid (in a 1:2 molar ratio) prior to addition to 16-AP. The fluorescence intensity of bound 16-AP again was diminished in intensity by about 30%. Thus, competition between 16-AP and 22:6 fatty acid for a binding site or the close proximity of such sites could be a possible explanation for our observation. A more extensive analysis using different fatty acids would be necessary to quantify such a competition.

Spectroscopic Properties of IRBP-Bound AOffa. The absorption and emission characteristics of different AOffas after binding to IRBP were generally similar. A difference, however, in the magnitude of a blue shift in emission maxima was observed. Typical absorption and emission spectra are shown for 2-AP in Figure 5. There is an approximately 3-fold

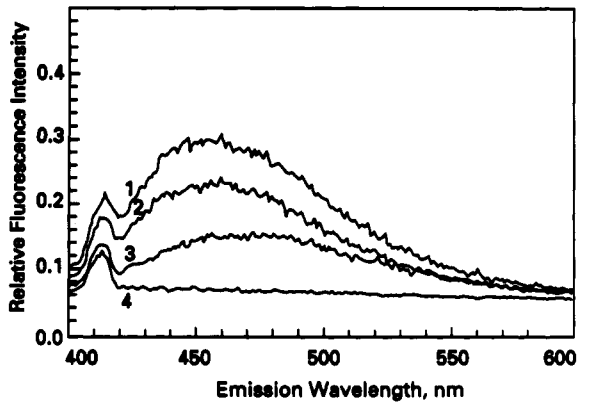

FIGURE 4: Effect of DHA (22:6) on relative fluorescence intensity of 16-AP. Emission spectra of 16-AP bound to IRBP (1), 16-AP bound to IRBP in the presence of DHA (2), free 16-AP (3), and IRBP in PBS buffer (4) are shown. Concentrations were as follows: IRBP, 0.6 μM; 16-AP, 1.2 μM; DHA, 1.2 μM.

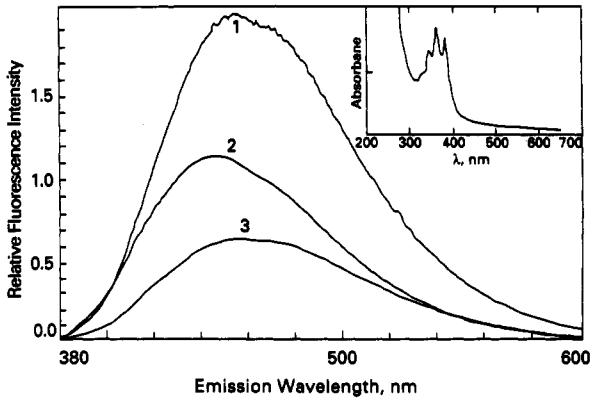

FIGURE 5: Emission spectra of 2-AP bound to IRBP (1), 2-AP bound to IRBP in the presence of acrylamide (2), and 2-AP in PBS (3). Wavelength of excitation was 360 nm. Concentrations of 2-AP, IRBP, and acrylamide were 400, 200, and 500 nM, respectively. Inset: absorption spectrum of 2-AP in PBS.

increase in the fluorescence intensity of 2-AP upon binding to IRBP and the maximum of emission, i.e., the wavelength of maximal fluorescence is blue-shifted from 460 to 454 nm (curves 1 and 3, Figure 5). The blue shift is even more pronounced in the presence of a quencher (line 2, Figure 5).

The size of the blue shift varies with the position of the anthroyloxy moiety on the stearic acid analog and increases toward the midpoint of the carbon chain (Figure 6A). Variation of the quantum yield with the attachment site is also observed (Figure 6B). In general, the values for quantum yield indicate that AOffas are bound to IRBP in a hydrophobic environment. The most significant decrease in the quantum yield is observed around the C-10 region where it reaches the lowest value (Q = 0.05). Such a low quantum yield value could be due to a polar environment, e.g., the close proximity of a charged amino acid.

Nonradiative Energy Transfer. Energy transfer from tryptophan residues to bound OAffa was monitored by the decrease in the intensity of tryptophan fluorescence. As can be seen from Figure 7, there is a decrease in tryptophan fluorescence (donor) with a corresponding increase in 16-AP fluorescence (acceptor) upon binding of this ligand. The efficiency of transfer was calculated to be E = 0.19. There are 11 tryptophan residues in bovine IRBP (Borst et al., 1889), which allows for multiple donor energy transfer. The calculated efficiency of transfer (Table II) thus represents the average of efficiencies for all distances involved (Lakowicz, 1983); no attempt was made to evaluate a possible distribution

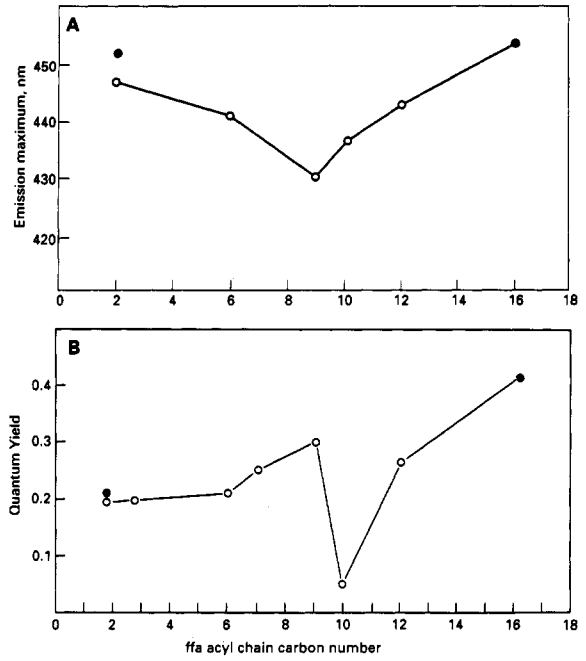

FIGURE 6: Effect of position of anthroyloxy group on (A) maximum fluorescence emission of fluorescent fatty acid analogs bound to IRBP and (B) quantum yield of fluorescent fatty acid analogs bound to IRBP. Excitation wavelength was 30 nm. Open circles, data points for stearic acid derivatives; filled circles, data points for palmitic acid derivatives.

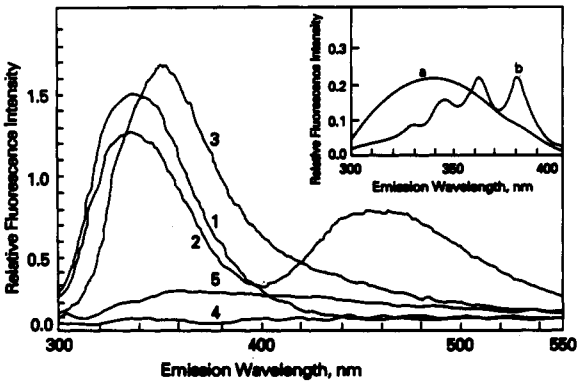

FIGURE 7: Emission spectra of tryptophan fluorescence in IRBP. Wavelength of excitation was 295 nm. The buffer used in all cases was PBS, pH 7.2. Curve 1, 100 nM IRBP alone; curve 2, 100 nM IRBP with 200 nM 16-AP; curve 3, 100 nM IRBP and 200 nM 16-AP with 6.7 M urea; curve 4, buffer alone; curve 5, 6.7 M urea in buffer. Inset: Overlap of normalized emission spectrum of tryptophan (a) and absorption spectrum of 16-AP (b).

Table II: Energy Transfer Efficiencies from Tryptophan Residues to Bound AOffa

AOffa	*E*	AOffa	*E*
2-AS	0.07	9-AS	0.22
2-AP	0.11	12-AS	0.10
6-AS	0.20	16-AS	0.17

of these distances.

The efficiency of nonradiative energy transfer from tryptophan in IRBP to bound 16-AP is sensitive to conformational changes in the protein induced by urea. Curves 2 and 3 of Figure 7 present the emission spectra of tryptophan residues in IRBP with a bound ligand in the presence and the absence of urea. The emission maximum at 460 nm (curve 2) is due to energy transfer from tryptophan residues to bound fatty acid. On exposure to urea (curve 3), no emission at 460 nm could be observed. The maximum and quantum yield of

Table III: Energy Transfer Efficiencies from Tryptophan Residues to Bound 16-AP in the Presence of Urea

[urea] (M)	*E*
0	0.17
1.3	0.26
2.7	0.14
4	0.06
6.7	0.07

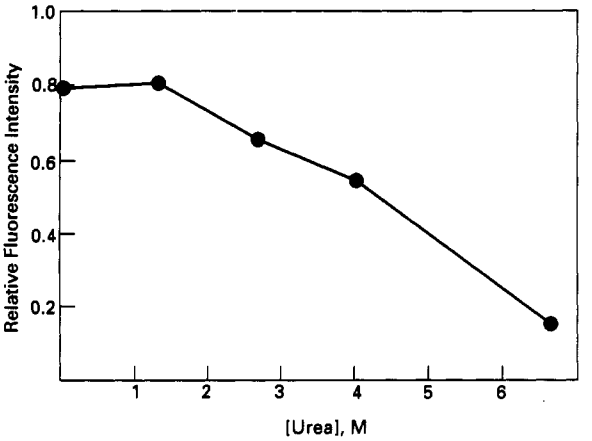

FIGURE 8: Effect of urea on the interaction of 16-AP with IRBP as assessed by fluorescence intensity of bound fluorophore. Wavelengths of excitation and emission were 360 and 454 nm, respectively. Data are corrected for emission due to urea and free fluorophore.

tryptophan fluorescence are typical for a denatured protein (Lakowicz, 1983). Table III presents the efficiencies of energy transfer from tryptophan residues to a bound ligand at different urea concentrations. As can be seen, the efficiency of energy transfer is slightly increased at a low concentration of urea but progressively diminishes as the concentration of denaturant increases.

Effect of Urea on Aoffa–IRBP Interactions. Fluorescence maxima of tryptophan residues in proteins reflect the degree of tryptophan exposure to a solvent (Lakowicz, 1983). Fluorescence maximum of tryptophan fluorescence in IRBP on exposure to urea is red-shifted (Figure 7), indicating the unfolding of protein by the denaturant. If ligand binding sites are dependent on specific constraints of secondary structure, urea disruption of IRBP conformation should decrease fatty acid binding. As seen in Figure 8, fluorescence intensity of bound AOffa, which is the indicator of protein–ligand interactions, decreases in the presence of increasing concentrations of denaturant. Corrections for the effect of urea on AOffa and IRBP fluorescence were applied. There is a small increase in fluorescence intensity with the addition of 1.3 M urea, but with further increases in concentration, a marked decline in fluorescence intensity is observed. AOffa–IRBP interactions are thus sensitive to the conformational changes induced by urea.

Fluorescence Quenching. Acrylamide is a small neutral quenching molecule which can diffuse through the protein matrix. We examined the microenvironment of the fatty acid binding site by probing its accessibility to the acrylamide quencher molecule. The results are presented in Figure 9 and are plotted according to the Stern–Volmer equation (Lakowicz, 1983). The Stern–Volmer equation describes the collisional mechanism of quenching due to diffusion of a quencher through the protein matrix. As is apparent from the family of curves, the anthroyloxy moieties of AOffa are in different microenvironments within the binding site as judged by accessibility to the quencher. Values for quenching constants are presented

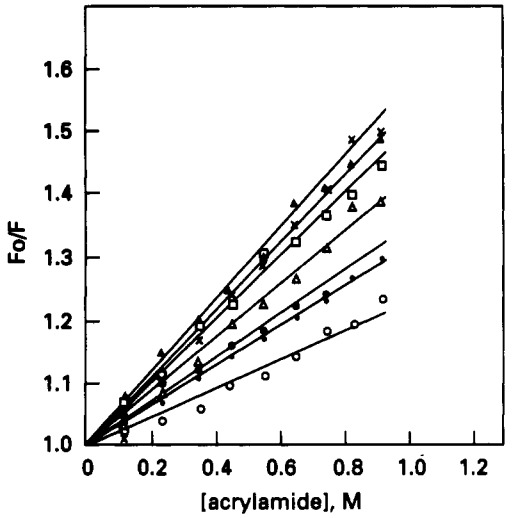

FIGURE 9: Stern–Volmer plots of fluorescence quenching of AOffa bound to IRBP by acrylamide. Probes used were 2-AS (▲), 12-AS (×), 6-AS (□), 3-AS (△), 9-AS (●), 7-AP (•), and 16-AP (○). Values are from one of three replicate experiments. Wavelengths of excitation and emission were 360 and 454 nm. Lines represent least-squares fit.

Table IV: Stern–Volmer Quenching Constants[a]

AOffa	K_{SV}	AOffa	K_{SV}
2-AS	0.599	9-AS	0.333
3-AS	0.410	10-AS	nd
6-AS	0.500	12-AS	0.552
7-AS	0.300	16-AP	0.272

[a] Constants (K_{SV}) were calculated from data in Figure 9 for the different analogs. nd, not determined.

in Table IV and indicate that the midportion of AOffa is less accessible to quencher molecules. This is consistent with the emission maxima data in that the more hindered residues also are less accessible to the diffusing acrylamide. The Stern–Volmer quenching constant could not be determined for the C-10 area due to the very low values of quantum yield of bound 10-AS.

DISCUSSION

Excellent use of analogs has been made in recent years to probe fatty acid binding site microenvironments in a number of fatty acid binding proteins (Storch, 1989; Storch et al., 1990; Wootan et al., 1990; Peeters et al., 1989). While it is not possible to rule out the potential influence of the fluorescent moiety on the absolute parameters of fatty acid–protein interactions, it is possible to use these probes for a comparative characterization. Importantly, the binding stoichiometry and affinities obtained for the AOffas are comparable to the values for native free fatty acids (Veerkamp et al., 1987). We have used a set of anthroyloxy fatty acid isomers and homologs as fluorescent probes to examine the fatty acid binding site(s) in IRBP. The intrinsic fluorescent properties of these probes are independent of the AO covalent attachment site (Thulborn et al., 1978; Huang et al., 1988). Therefore, by using a set of fatty acids with the fluorescent moiety attached at different positions along the carbon chain, it is possible to compare a microenvironment within a different parts of a binding site.

The number of binding sites and apparent dissociation constants were evaluated for two AOffas: 16-AP and 9-AS. Analysis of binding data using a Cogan plot indicates that IRBP contains a single specific binding site with a stoichiometry of 1:1 and dissociation constant of about 3.6×10^{-7} M. The apparent dissociation constants are of the same magnitude as for the FABPs of liver and heart as well as for serum albumin (Peeters et al., 1989). The dissociation constant for retinol binding to IRBP has been determined by Adler et al. (1985) to be 1.3×10^{-6} M; this is about 30-fold lower then the dissociation constants for AOffa. Preliminary results of studies on competition between *all-trans*-retinol and palmitic acid (Hazard et al. 1991) suggest a possible interrelation between these ligands on binding to IRBP. Nonspecific binding to IRBP at high exogenous ligand concentrations was also observed for retinol (Adler et al., 1985). It is possible to speculate that IRBP binds ligands such as retinol and fatty acids at specific sites and also can facilitate solubilization of a number of fatty acids by nonspecific hydrophobic adsorption. This assumption is in agreement with our previous finding that purified bovine IRBP does, in fact, carry a number of free fatty acids (Bazan et al., 1985).

The emission characteristics of AOffas change on binding to IRBP and their variations indicate a highly organized binding site. The position of emission maxima of AOffa fluorescence is sensitive to steric hindrance because the rotational constraint upon the anthracene ring prevents inner-system relaxation so that the resulting emission occurs from a higher energy state and is, therefore, blue-shifted (Matayoshi et al., 1981; Storch et al., 1989). The variations in quantum yield observed with the analogs differing in their anthroyloxy (AO) attachment site indicate differential polarity within the AOffa binding site (Thulborn et al., 1987). As can be seen from Figure 5, bound 2-AP (curve 1) is characterized by about a 3-fold increase in fluorescence emission and a blue shift in emission maximum to 454 nm. As seen in the plot of quantum yield values as a function of AO attachment site, the values are highest for probes with the fluorophore attached close to the methyl end of the fatty acid; this indicates a nonpolar environment. Quantum yield values for AO moieties near the carboxyl end are much lower, indicating an environment of higher polarity. Deviation from this trend is pronounced near the C-10 region of the fatty acid chain, where the quantum yield of bound AOffa drops to its lowest value (Figure 6B). Since the emission maxima data show that there is considerable motional constraint at this part of the binding site (Figure 6A), the very low quantum yield value would be indicative of a close proximity to charged amino acids rather than exposure to the aqueous phase. In any case, such fluctuations reflect fine structure within the IRBP binding site in terms of polarity gradients of the protein matrix. Fluorescence studies of quantum yield changes seen with AOffa binding to other FABPs also show considerable variation with AO attachment site (Wootan et al., 1990; Storch et al., 1989).

Nonradiative energy transfer between two fluorophores occurs due to dipole–dipole interaction during the excited state, provided that the emission of one fluorophore overlaps the absorption of another (Lakowicz, 1983). Figure 7 demonstrates the overlap of the emission spectrum of tryptophan in IRBP and the absorption spectrum of 16-AP (inset) and also demonstrates a decrease in tryptophan fluorescence (donor) in the presence of bound 16-AP (acceptor). The highest values for energy transfer are observed for the midportion of the AOffa carbon chain (Table II). This is consistent with other fluorescence characteristics, adding weight to our supposition that the midportion of AOffa is submerged deeper into the protein matrix than the carboxyl or methyl ends. Since there are multiple tryptophan residues in IRBP that can participate in energy transfer and since the Förster theory is only applicable to a single donor–acceptor pair, our observations reflect the

overall distribution of a number of distances. While it would be informative to be able to resolve single distances, these energy transfer data are viewed in terms of the relative comparison of changes in average distance distribution and not the specific distances involved. The usefulness of such an approach is illustrated with data from Table III. At concentrations of urea above 4 M there is a major redistribution of donor–acceptor distances. It is of interest to note that, at low denaturant concentrations (up to 1.3 M urea), there is an increase in efficiency of transfer which could be due to a local increase in hydrophobicity induced by the denaturant. Although we cannot quantitatively correlate these changes to the conformational changes induced by urea, these data, together with the data on tryptophan emission maxima, clearly indicate changes in the overall architecture of the protein molecule on exposure to increasing concentrations of urea. Do these changes affect the fatty acid binding site? Figure 8 illustrates the effect of urea on AOffa–IRBP interaction. Fluorescence intensity of bound 16-AP decreases with an increase in urea concentration. But fluorescence intensity, i.e., a quantum yield, is dependent on the local polarity within a binding site. In view of energy transfer and emission maxima data and the fact that urea itself is a neutral molecule, we conclude that the stoichiometry of the fatty acid binding site is affected by urea.

Acrylamide is an effective quencher commonly used to probe the microenvironments of intrinsic and extrinsic fluorophores in proteins (Lakowicz, 1983). Quenching of fluorescence may occur by several mechanisms (Lakowicz, 1983). In the case of collisional quenching, fluorescence intensities are quenched in proportion to the quencher concentration and depend on the diffusion rate of the quencher through a protein matrix. Quenching of the fluorophore may also occur by a static process which results in an exponential increase in I_o/I with quencher concentration. We used a neutral quencher, acrylamide, to evaluate the location of the probe relative to the architecture of the IRBP binding site. In our studies, no significant exponential dependence was observed, and we have analyzed the quenching data determining the K_{SV} using the Stern–Volmer equation for collisional quenching. A K_{SV} value could not be calculated for 10-AS due to an extremely low quantum yield of this probe when bound to IRBP. All IRBP-bound AOffas we have tested are accessible to acrylamide. There is considerable variation in K_{SV} with the positioning of the AO moiety, indicating that the binding site is a highly organized structure. As seen from Table IV, the least accessible probe is 16-AP; this correlates well with the fact that this probe demonstrates the highest quantum yield upon binding to IRBP. Lowest values were obtained for a fluorophore with attachment site at the midportion of the carbon chain (7-AS and 9-AS). Data on the emission maxima suggest that this part of the AOffa is under considerable steric hindrance, which could explain the poor accessibility to quencher. Fluorophores at the carboxyl end have much higher values of K_{SV}. Quantum yield data together with emission maxima positions indicate that these residues are in a more polar and less constrained location; therefore, the rate of acrylamide diffusion, and hence its concentration and frequency of collision, would be higher for those residues. Quenching data for FABPs also demonstrate a highly structured binding site with a critical interaction possibly through the midportion of the carbon chain (Wootan et al., 1989; Storch et al., 1989). Overall, the collected data point to a highly rigid architecture of both the IRBP and FABP binding sites that primarily involves the C-10 AOffa area. One may speculate that such a binding site could accommodate a variety of free fatty acids of different lengths through specific interactions over a relatively short portion of the carbon chain.

In summary, we have shown that IRBP has a specific site to bind fatty acids with relatively high affinity that shows a structure similar to sites observed with other, well-known, fatty acid-binding proteins (Wootan et al., 1990; Storch et al., 1990). This is actually somewhat surprising since IRBP is so dissimilar in amino acid sequence to the FABPs and does not belong to the FABP gene family. Because of IRBP abundance, ease of purification, and the apparent similarity of its binding site to that of the FABPs, it thus offers a potentially excellent model for studying free fatty acid binding characteristics. Since photoreceptor membranes are highly enriched in specific fatty acids such as DHA, a protein carrier such as IRBP could be important in free fatty acid movement from pigment epithelial (PE) to visual cells. In the circadian process of disc shedding and subsequent phagocytosis by PE cells (La Vail, 1976), retrieval of important components such as fatty acids from the PE and recycling across the IPM back to the retina may require a protein carrier mediator. IRBP is thus ideally situated to facilitate two-way movement of free fatty acids across the extracellular space since it exhibits both a single, higher affinity binding site as well as a number of lower affinity sites that could facilitate bulk, relatively nonspecific flow. Finally, the extremely high concentration of IRBP in the IPM (Pfeffer et al., 1983) and its potential for binding multiple hydrophobic ligands could be of physiological importance in protecting free fatty acids in transit, much as has been proposed for retinoids (Crouch et al., 1992).

ACKNOWLEDGMENT

We thank Dr. S. Gentleman for the critical review of the manuscript.

REFERENCES

Adler, A. J., & Spencer, S. A. (1991) *Exp. Eye Res. 53*, 337–346.

Adler, A. J., Evans, C. D., & Strafford, W. F. (1985) *J. Biol. Chem. 260*, 4850–4855.

Bazan, N. J., & Reddy, T. S. (1985) *Handb. Neurochem. 8*, 507–575.

Bazan, N. G., Reddy, T. S., Redmond, T. M., Wiggert, B., & Chader, G. J. (1985) *J. Biol. Chem.* **260**, 13677–13680.

Benelken, R. M., Anderson, R. E., & Wheeler, T. G. (1973) *J. Neurosci. Res. 18*, 591–596.

Berman, E. R. (1991) *Biochemistry of the Eye*, pp 376–379, Plenum Press, New York.

Borst, D. E., Redmond, T. M., Elsner, J. E., Gonda, M. A., Wiggert, B., Chader, G. J., & Nickerson, J. M. (1989) *J. Biol. Chem. 264*, 1115–1123.

Carlson, A., & Bok, D. (1992) *Biochemistry 31*, 9056–9062.

Chaplin, D. B., & Kleinfeld, A. M. (1983) *Biochim. Biophys. Acta 731*, 465–474.

Cogan, U., Kopelman, M., Mokady, S., & Shinitsky, M. (1976) *Eur. J. Biochem. 65*, 71–78.

Crouch, R. K., Hazard, E. S., Lind, T., Wiggert, B., Chader, G. J., & Corson, W. (1992) *Photochem. Photobiol. 56*, 251–255.

Dowling, J. (1960) *Nature 188*, 114–118.

Fong, S. L., Lion, G. I., Landers, R. A., Alvarez, R. A., & Bridges, C. D. (1984) *J. Biol. Chem. 259*, 6534–6542.

Hazard, E. S., Crouch, R. K., Chader, G., & Wiggert, B. (1991) *Invest. Opthalmol. Visual Sci. Suppl. 33*, 1250.

Huang, N., Casteel, F. K., & Feigonson, G. W. (1988) *Biochim. Biophys. Acta 939*, 124–130.

Gery, I., Wiggert, B., Redmond, T. M., Kuwabara, T., Crawford, M. A., Vistica, B. P., & Chader, G. J. (1986) *Invest. Ophthalmol. Visual Sci. 27*, 1296–1300.

Glatz, J. F. C., & Vusse, G. J. (1990) *Mol. Cell. Biochem. 98*, 237–251.

Lai, Y.-L., Wiggert, B., Liu, Y., & Chader, G. J. (1982) *Nature 298*, 848–849.

Lakowicz, J. R. (1983) *Principles of Fluorescence Spectroscopy*, pp 257–274, Plenum Press, New York.

La Vail, M. M. (1976) *Science 194*, 1071–1073.

Martin, M. E., Vranckx, R., Benassayag, C., & Nunez, E. A. (1986) *J. Biol. Chem. 261*, 2954–2959.

Matayoshi, E. D., & Kleinfeld, A. M. (1981) *Biophys. J. 35*, 212–235.

Okajima, T. L., Pepperberg, D. R., Ripps, H., Wiggert, B., & Chader, G. J. (1989) *Exp. Eye Res. 49*, 629–644.

Okajima, T. L., Pepperberg, D. R., Ripps, H., Wiggert, B., & Chader, G. (1990) *Proc. Natl. Acad. Sci. U.S.A. 87*, 6907–6911.

Peeters, R. A., Groen, M. A. P. M., de Moel, M. P., van Moerkerk, H. T. B., & Veerkamp, J. H. (1989) *Int. J. Biochem. 21*, 407–418.

Pepperberg, D. R., Okajima, T. L., Ripps, H., Chader, G. J., & Wiggert, B. (1991) *Photochem. Photobiol. 54*, 1057–1060.

Pfeffer, B., Wiggert, B., Lee, L., Zonnenberg, B., Newsome, D., & Chader, G. J. (1983) *J. Cell. Physiol. 117*, 333–341.

Saari, J. C., Teller, D. C., Crabb, J. W., & Bredberg, L. (1985) *J. Biol. Chem. 260*, 195–201.

Sani, B. P., Allen, R. D., Moorer, C. M., & McGee, B. W. (1987) *Biochem. Biophys. Res. Commun. 147*, 25–30.

Scott, T. G., Spencer, R. D., Leonard, N. J., & Weber, G. (1970) *J. Am. Chem. Soc. 92*, 687–695.

Storch, J. (1990) *Mol. Cell. Biochem. 98*, 141–147.

Storch, J., Bass, N. M., & Kleinfeld, A. M. (1989) *J. Biol. Chem. 264*, 8708–8713.

Thulborn, K. R., & Sawyer, W. H. (1978) *Biochim. Biophys. Acta 511*, 125–140.

Vallette, G., Vanet, A., Sumida, C., & Nunez, E. A. (1991) *Endocrinology 129*, 1363–1369.

Veerkamp, J. H., & Paulussen, R. J. A. (1987) *Biochem. Soc. Trans. 15*, 331–336.

Werner, T. C. (1976) in *Modern Fluorescence Spectroscopy*, pp 277–317, Plenum Publishing, New York.

Wootan, M. G., Bass, N. M., Bernlohr, D. A., & Storch, J. (1990) *Biochemistry 29*, 9305–9311.